For the same jet chamber pressure at Mach 2.0, the single, sonic jet produced higher amplification factors per pound of mass injected than the four-diverter fluidic jet system. Jet interaction amplification factors were also larger per pound of gas injected for helium than they were for air or nitrogen at the same chamber pressure for the conditions tested. However, both jets and all gases produced the same amplification when compared on a momentum basis.

The flow pattern and pressure behind the fluidic jet very much resembled the classical two-dimensional base flow phenomenon.

References

[1] Spaid, F. W., Zukoski, E. E., and Rosen, R., "A Study of Secondary Injection of Gases Into a Supersonic Flow," TR 32-834, Aug. 1966, Jet Propulsion Lab., California Institute of Technology, Pasadena, Calif.

[2] Cassel, L. A., Davis, J. G., and Engh, D. P., "Lateral Jet Control Effectiveness Prediction for Axisysmmetric Missile Configurations," Rept. RD-TR-68-5, June 1968, U. S. Army Missile Command, Redstone Arsenal, Ala.

[3] Kaufman, L. G., "Interaction Between High Speed Flows and Transverse Jets: A Method for Predicting the Resultant Surface Pressure Distribution," Rept. RE-348A, April 1969, Grumman Aircraft Engineering Corp., Bethpage, N. Y.

[4] Werle, M. J., "A Critical Review of Analytical Methods for Estimating Control Forces Produced by Secondary Injection," NOLTR 68-5, Jan. 1968, U. S. Naval Ordnance Lab., White Oak, Md.

[5] Koch, L. S. and Collins, D. J., "The Effect of Varying Secondary Mach Number and Injection Angle on Secondary Gaseous Injection Into a Supersonic Stream," AIAA Paper 70-552, Tullahoma, Tenn., 1970.

[6] Dahm, T. J., "The Development of an Analogy to Blast Wave Theory for the Prediction of Interaction Forces Associated with Gaseous Secondary Injection into a Supersonic Stream," TN 9166-TN-3, May 1964, Vidya Corp., Palo Alto, Calif.

[7] Cassel, L. A. et al., "Jet Interaction Control Effectiveness for Subsonic and Supersonic Flight," Rept. RD-TR-69-21, Sept. 1969, U. S. Army Missile Command, Redstone, Arsenal, Ala.

[8] Kupier, R. A., "Control Jet Effectiveness in the Subsonic and Transonic Regimes," Rept. U-2932, Dec. 1964, Philco Aeronautic Div. of the Ford Motor Co., Newport Beach, Calif.

[9] Wolfe, J. A., "High Speed Wind Tunnel Handbook," LTV Publication AFR-EIR-13552-A, June 1968, LTV Aerospace Corp., Dallas, Texas.

APRIL 1971 J. SPACECRAFT VOL. 8, NO. 4

Thermal Radiation Absorption by Particle-Seeded Gases

J. R. Williams,* W. L. Partain,† A. S. Shenoy,‡ and J. D. Clement§
School of Nuclear Engineering, Georgia Institute of Technology, Atlanta, Ga.

Particle-seeded gases are currently being considered as propellants for gas core nuclear rocket engines and for other applications such as thermal shielding for re-entry vehicles and rocket nozzle cooling which require that surfaces be protected from intense thermal radiation. To evaluate radiant heat transfer through a particle-seeded gas, one must know the extinction parameter, the scattering parameter, and the scattering amplitude function of the particles. The extinction parameters of submicron particles dispersed in hydrogen at 1 atm pressure have been measured as a function of wavelength from 1200 to 6800 Å at various temperatures to 2170°K and are ~50,000 cm²/g for carbon, ~20,000 cm²/g for tungsten, and ~65,000 cm²/g for silicon. The extinction parameter of submicron tungsten particles in hydrogen at 12.5 atm showed an increase to ~50,000 cm²/g as the temperature was raised to 2030°K, and at 100 atm it reached ~100,000 cm²/g at 2300°K. The scattering amplitude functions of submicron carbon, tungsten, silicon, tungsten carbide, and silicon carbide dispersed in nitrogen were measured and scattering from these particles was shown to be highly forward, that is, most of the scattered light is scattered at angles <30°.

Nomenclature

I = intensity of a beam of radiant energy
j = emission coefficient
k = linear attentuation coefficient
p = scattering amplitude function
s = distance variable
x = path length through a particle cloud
θ = angle of scattering
λ = wavelength
μ_a = absorption parameter
μ_e = extinction parameter
μ_s = scattering parameter
ρ = mass of particles per unit volume of aerosol
Ω,Ω' = solid sngles

Received February 6, 1970; presented as Paper 70-838 at the AIAA 5th Thermophysics Conference, Los Angeles, Calif., June 29–July 1, 1970; revision received December 14, 1970. The research described in this paper was supported by NASA grant NGR-11-002-068 and administered by the Nuclear Systems Division of the NASA Lewis Research Center. The authors would like to thank W. R. Jacobs, an AEC Fellow in the School of Nuclear Engineering, for his work on the scattering measurements. The authors especially appreciate the many helpful suggestions given them by C. Masser of the Nuclear Systems Division of the NASA Lewis Research Center.

* Assistant Professor. Member AIAA.
† Research Assistant.
‡ Research Engineer; presently with the Gulf General Atomic Corp.
§ Professor.

Introduction

THE absorption of thermal radiation by a gas is usually greatly enhanced by the dispersion of small metallic particles in the gas. The particles absorb radiant energy and

heat the gas by conduction. If the particles are small enough, they usually remain essentially in thermal and dynamic equilibrium with the gas. A seeded propellant layer next to the inner wall of a rocket nozzle can reduce the radiant heat flux at the nozzle wall by two orders of magnitude.[1] Gas-core reactor concepts for nuclear rocket propulsion[2–4] rely on radiant heating of particle-seeded hydrogen in order to achieve the desired high propellant temperatures. Such reactors are also being considered as a heat source for large, highly efficient electric power stations using an MHD topping cycle.[5–7] Such a system may use particle-seeded argon as the working fluid, which would be heated in the reactor by thermal radiation from the hot, fissioning uranium core. An absorbing layer of particle-seeded air may also be used for shielding re-entry vehicles.[8] For all of these applications, the particles should be strongly absorbing in the ultraviolet, visible, and near infrared and should withstand high temperatures without reacting or vaporizing. Submicron-sized particles of refractory metals generally satisfy both requirements.

Lanzo and Ragsdale[9] made tests by radiating energy from an electric arc to unseeded air, and to air that contained submicron-sized carbon particles, in an annular heat exchanger. Whereas the unseeded air temperature reached 556°K the seeded air stream reached 667°K. Keng and Orr[10] reported theoretical and experimental studies of radiant heat transfer from a heated tungsten cylindrical enclosure to unseeded or seeded helium within it. Helium was passed through the tube, and the tube dimensions and helium flow rate were selected to give a low thermal efficiency for forced convection heating; the addition of tungsten or carbon particles caused a significant increase in heat absorption. Burkig[11] measured the absorption by injecting an aerosol into a transparent quartz tube and exposing it to a flash of a xenon flash tube. The temperature rise of the gas was inferred from the pressure

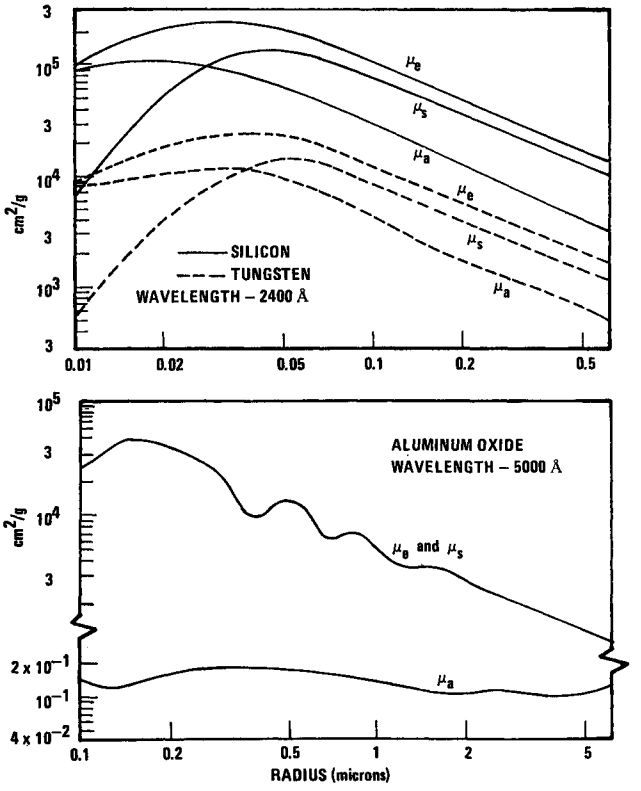

Fig. 1 Extinction, absorption, and scattering parameters of submicron refractory particles calculated using the Mie theory (data for AlO taken from Ref. 19).

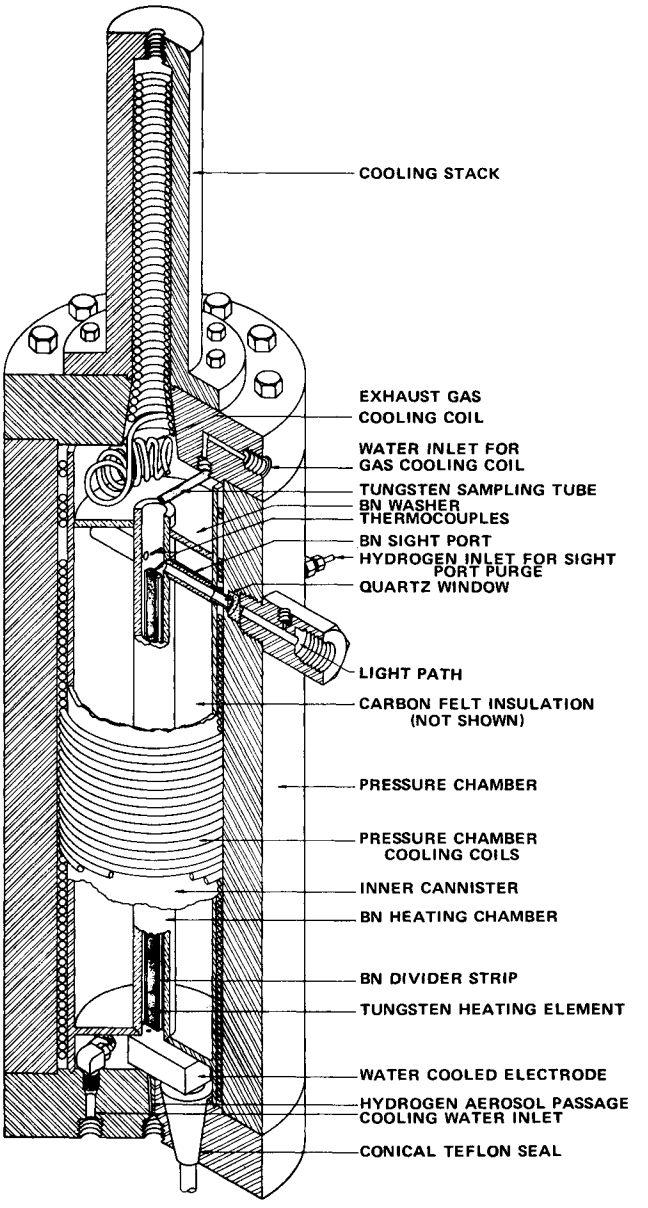

Fig. 2 High-pressure furnace assembly.

rise measured with a fast response pressure transducer. The bulk of the work was with micron-sized particles of carbon, iron, and tantalum carbide. In general, initial pressures of 2 and 5 atm were investigated for both He and H_2. During the flash the aerosol temperature rose to ~3000°K or more for ~1 msec. Klein and Roman[12] have recently studied radiant heating of carbon seeded argon by flowing the aerosol around a high-power d.c. arc. Unseeded buffer layers were used to prevent coating of the transparent duct walls. Aerosol temperatures as high as 2200°K were attained at a pressure of 1 atm.

The scattering amplitude function and extinction parameter of micron-sized aluminum oxide particles was reported by Love[13] for wavelengths in the infrared region between 4 and 16 μ. Williams[14] measured the intensity of He-Ne laser light scattered from submicron-sized particles of tungsten, carbon, silicon, tungsten carbide, and silicon carbide over a 30° angle and verified the forward nature of the scattering.

For the first time, the extinction parameter of submicron refractory particles dispersed in hydrogen has been measured at high temperatures and pressures over a broad wavelength

range. These data are particularly useful for evaluating the heat deposited in the propellant of gas core nuclear rocket engines.

The roles that the extinction parameter, the scattering parameter, and the angular scattering function play in thermal radiation transport are easily seen if one writes the equation for steady state thermal radiation transport through a transparent gas seeded with particles

$$\frac{1}{\rho}\frac{dI(\lambda,\Omega)}{ds} = -\mu_e(\lambda)I(\lambda,\Omega) + j(\lambda) + \mu_s(\lambda)\int_0^{4\pi} I(\lambda,\Omega')p(\lambda,\cos\theta)\frac{d\Omega'}{4\pi}$$

where I = the intensity of radiant energy in a unit wavelength interval at λ traveling in direction Ω, s = distance, Ω = solid angle, j = emission coefficient, p = scattering amplitude function, and θ = angle of scattering. It is seen that $\mu_e(\lambda)$, $\mu_s(\lambda)$, $p(\lambda, \cos\theta)$, and $j(\lambda)$ should be known over the applicable temperatures and wavelength ranges, and $p(\lambda, \cos\theta)$ should be known for scattering angles from 0 to 180°.

A rigorous solution to Maxwell's equations for the absorption and scattering of radiant energy by homogeneous spherical particles of any composition suspended in a homogeneous nonmagnetic transparent medium was published in 1908 by Gustav Mie[15] and is now commonly known as the Mie theory. Krascella[16] applied a transformation procedure developed by Aden[17] to the Mie equations to calculate the effect of particle size, wavelength, and particle temperature on the extinction, absorption, and scattering parameters of refractory particles in those regions of the ultraviolet, visible, and infrared spectra for which complex index of refraction data were available. The authors used Krascella's program to extend these calculations over a broader wavelength range.[18] The Mie theory predicts that $\mu_a(\lambda)$ is a maximum when the particle radius is of the order of the wavelength λ divided by 2π. Thus, for a given particle seed density ρ, the absorption of thermal radiation in the near infrared, visible, and ultraviolet regions of the spectrum is greatest for submicron-sized particles of diameters in the range of 0.05 to 0.50 micron. Submicron-sized particles of refractory materials are generally highly irregular in shape, so the Mie theory can only be used as an approximation to the absorption and scattering characteristics of these particles.

Calculations using the Mie theory require a knowledge of the particle radius, wavelength of the radiant energy, and the complex index of refraction of the spherical particles. The real part of the refractive index is believed to vary slowly with temperature, although experimental data at temperatures other than room temperature are quite limited. Some results of Mie theory calculations[18,19] are presented here to permit a comparison of the absorption characteristics of metallic and nonmetallic refractory particles (Fig. 1).

Highly absorbing particles, such as carbon, have a scattering parameter about equal to the absorption parameter when the particle diameter is large compared to the wavelength, and much smaller when the particles are small compared to the wavelength. Thus, carbon particles of very small sizes can be considered to be purely absorbing. Other metallic particles generally have scattering parameters several times higher than their absorption parameters but are purely absorbing for very small particle sizes. Nonconducting particles, such as magnesium oxide, aluminum oxide, or silica, have scattering parameters several orders of magnitude higher than their absorption parameters, so they scatter much more thermal radiation than they absorb. For any type of particle, the extinction parameter is a maximum for particles of diameters of the order of the wavelength divided by π.

Particles that are very small compared to the wavelength backscatter as much light as they scatter forward, and such scattering is symmetric about a scattering angle of 90°. This type of scattering is known as Rayleigh scattering. As the diameter is increased the scattering becomes more forward. The tendency of larger particles toward more highly forward scattering, when the particle diameters are of the same order of magnitude as the wavelength, is called the Mie effect. Particles that are large compared to the wavelength generally scatter in a very highly forward direction.

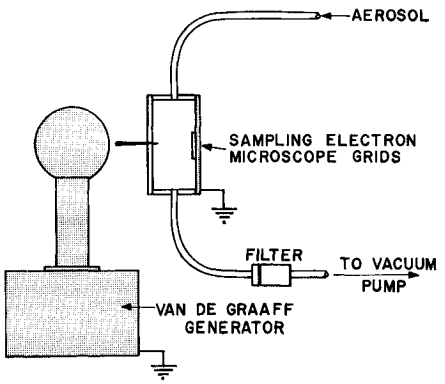

Fig. 3 Electrostatic aerosol sampling apparatus.

The angular scattering characteristics of particle clouds may have an important effect on radiant heat transfer through the cloud. Forward scattering particles are less effective in diffusing radiant energy than particles which tend to scatter energy at larger angles.

Measurements of the Extinction Parameter

If I_0 is the intensity of a radiant beam without the aerosol present, and I is the beam intensity after passing through a distance x of a gas containing ρ g/cm³ of particles, then

$$\mu_e = (1/\rho x)\ln(I_0/I)$$

μ_e is essentially independent of the composition of the carrier gas, provided that the carrier gas is transparent and there are no chemical reactions between the particles and the gas.

A beam of radiant energy was passed through hot hydrogen, first unseeded and then seeded, at a given temperature. Measurements of the transmitted energy for the two cases as a function of wavelength and simultaneous measurements of the aerosol density yielded the extinction parameter of the particle-seeded gas.

The high pressure furnace (Fig. 2) was designed to heat a flow of nonoxidizing gas to ~2800°K at pressures to 100 atm. The aerosol enters at the bottom of the furnace and passes into the boron nitride heating chamber which is insulated with carbon felt. The heating element is a 2.5 ft long by 0.62-in.-wide strip of 35-mil-thick tungsten whose ends are connected by copper leads to a 20 kw d.c. power supply. Supporting the tungsten heating element is a 0.125-in.-thick, hot-pressed BN strip.

Two sampling systems are used to simultaneously measure ρ by drawing known volumes of aerosol through filters. ρ is the mass of seed material deposited on the filter divided by the volume of gas that passed through. One sample is taken at the entrance of the furnace and the other is taken near the exhaust. These two samples are used to study the effect of temperature on seed vaporization as well as to evaluate μ_e.

Since submicron refractory metal particles contained in real aerosols are generally highly irregular in shape and exhibit a wide size variation, it is impossible to describe such aerosols by a single size parameter. In the opinion of the authors, the most useful description of the particles is a suitably prepared electron micrograph.

Several techniques were investigated for depositing the aerosol particles on the electron microscope grids so that the size distribution of the particles on the grids would be representative of that in the aerosol. The simplest approach is to

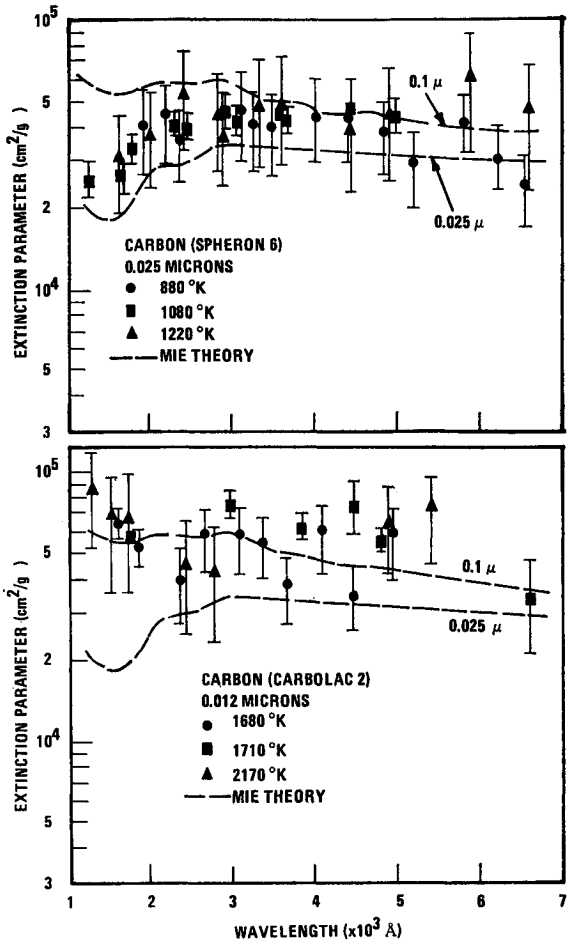

Fig. 4 Extinction parameter of carbon particles at 1 atm pressure.

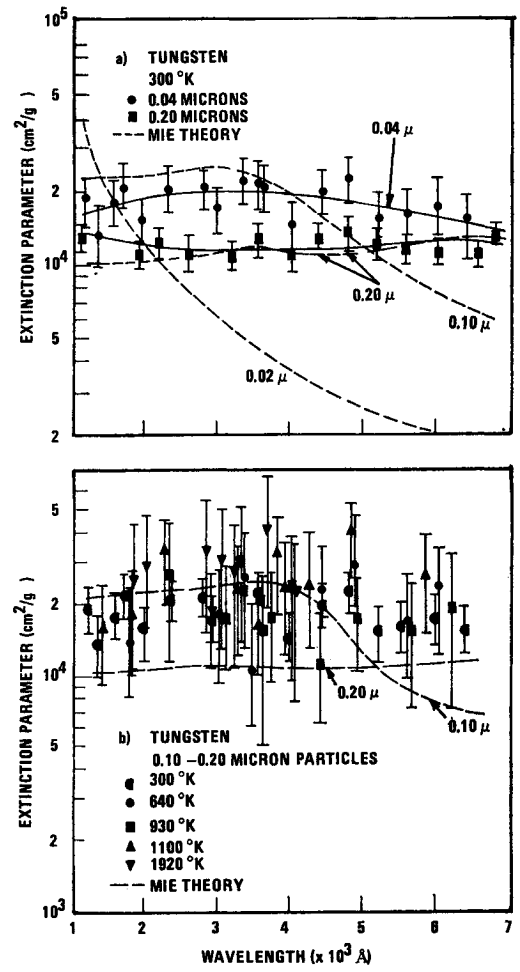

Fig. 6 Extinction parameter of tungsten particles at 1 atm pressure.

pass the grid through the aerosol stream, but it was felt that aerodynamic forces would favor the deposition of larger particles. Similarly, any approach based on allowing the particles to settle out on the grid would favor the larger particles and permit agglomeration. The technique employed to produce the electron micrographs utilized electrostatic precipitation (Fig. 3) to deposit the particles on the grids. A series of tests made with this apparatus showed that all of the particles were electrostatically removed from the aerosol stream and that there was no variation in the size distributions of particles deposited at different locations on the grounded metal plate opposite the Van de Graaff generator.

Well dispersed aerosols are difficult to obtain with low flow rates (~2 c.f.m. at standard temperature and pressure). Carbon aerosols were produced by mixing the gas and powder in a pressure vessel and exhausting the mixture through a 5-mil orifice. A high-speed food blender which was adapted for use in a pressure chamber produces satisfactory aerosols of carbon, silicon carbide, and silicon. A modified Wright dust generator was used to generate the tungsten aerosol.

Carbon was first used as a seed material due to its high absorption parameter, high sublimation temperature, and low neutron absorption cross section; μ_e was measured for Cabot Corporation Spheron 6 and Carbolac 2 carbon black in H_2 at 1 atm. Figure 4 shows μ_e for carbon (Spheron 6) as a function of λ at 880°, 1080°, and 1220°K. The dashed curves show μ_e for spherical carbon particles of 0.025 and 0.10 micron diameter as calculated using the Mie theory. Figure 4 also

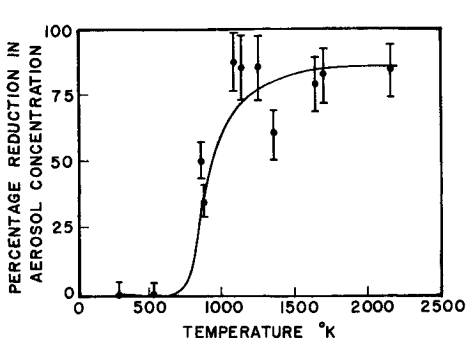

Fig. 5 Percentage reduction of carbon aerosol concentration after heating.

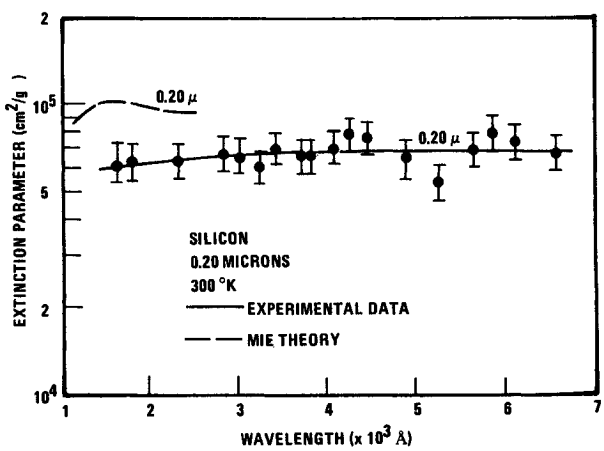

Fig. 7 Extinction parameter of silicon particles at 1 atm pressure.

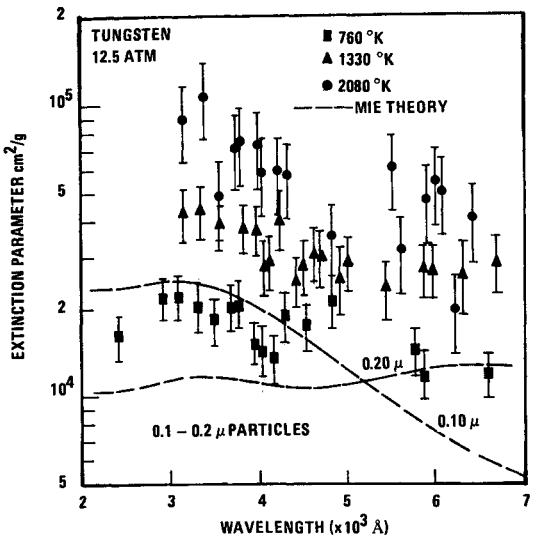

Fig. 8 Extinction parameter of tungsten particles at 12.5 atm pressure.

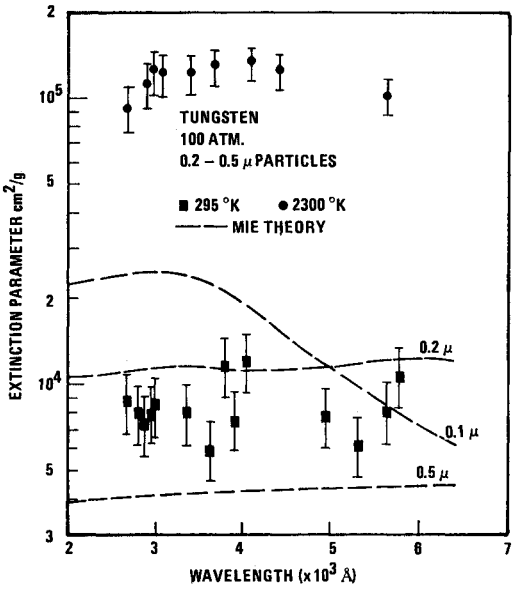

Fig. 10 Extinction parameter of tungsten particles at 100 atm pressure.

shows results for Carbolac 2. In both cases, the experimental values of μ_e are nearly independent of λ over the ranges of λ and T investigated.

It was found that ρ had to be increased tremendously in order to make attenuation measurements at higher temperatures because the decrease in ρ due to heating was much greater than that which would have been expected due to thermal expansion of the gas alone. It is thought that the additional seed material entering the furnace at higher temperatures serves to produce sufficient concentrations of the reaction products to slow down the reaction rate so that the remaining unreacted particles are observed when the attenuation is measured. The decrease in ρ (Fig. 5) was measured by taking simultaneous samples from the two ends of the furnace.

Very few data are available regarding chemical reactions of submicron refractory particles with hydrogen at elevated temperatures and pressures. Chi and Landahl[20] measured the weight loss and surface recession of graphite samples at pressures to 56 atm. and temperatures to 2800°K and found that methane and acetylene were the predominant products. If their reaction rate data were applied to a 0.05 μ diameter particle, the particle should react in ~1 sec at 2000°K and in ~0.01 sec at 2500°K. It has been shown, however (Fig. 5), that carbon particles of about that size react at much lower temperatures until significant reaction product concentrations are produced to retard the reaction rate. Others[21,22] have shown that the reaction rates and reaction product equilibria of carbon and other refractory materials with hydrogen depend strongly on pressure too.

In an effort to determine whether chemical reactions between carbon and hydrogen had taken place in our tests, a sample of the effluent from the furnace was passed through a water-cooled tube. After the mixture cooled, the carbon particles were separated both by an electrostatic precipitator and a fiber glass filter before the hydrogen was collected in the sampling tube. The sampling system was evacuated initially to remove traces of water and other gases. The collected sample was analyzed with a mass spectrograph. Strong peaks were observed for atomic numbers 15 and 16 (CH_3^+ and CH_4^+) confirming that some chemical reaction had occurred, because precautions had been taken to insure that there was

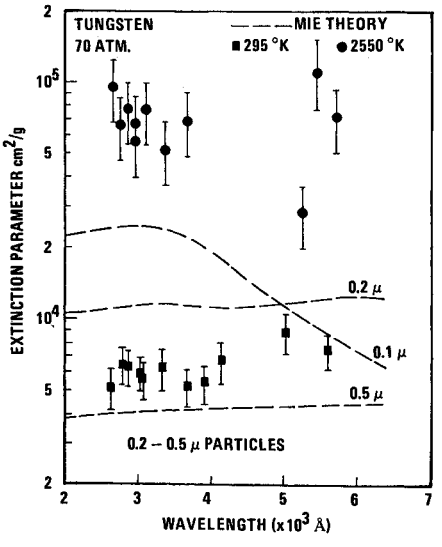

Fig. 9 Extinction parameter of tungsten particles at 70 atm pressure.

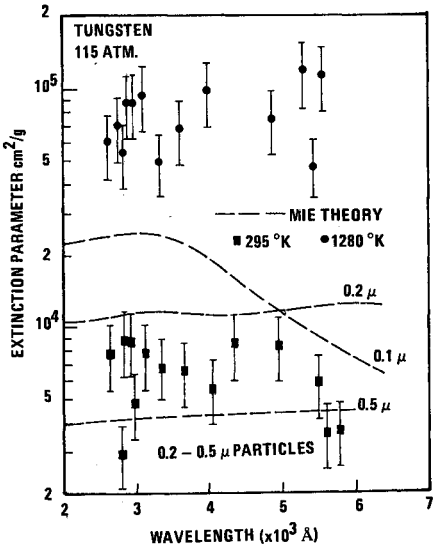

Fig. 11 Extinction parameter of tungsten particles at 115 atm pressure.

no methane contamination of the H_2, the carbon, or the apparatus.

The extinction parameters of 0.20 and 0.04 μ tungsten particles in H_2 at 300°K and 1 atm are presented in Fig. 6a together with theoretical values calculated for spherical tungsten particles of 0.02, 0.1, and 0.2 μ diameters using the Mie theory. Electron micrographs indicate that the tungsten particles are highly irregular in shape and are a mixture of different sizes.

As in the case of carbon, the measured μ_e of tungsten was essentially independent of λ for the conditions investigated. Its value is ~20,000 cm²/g, compared to 50,000 cm²/g for carbon. Figure 6b shows that there may be a small increase in μ_e for 0.04 μ minimum diameter tungsten at higher temperatures (1000°–1920°K). The theoretical extinction parameter is also plotted.

Results for submicron-sized silicon particles in H_2 at room temperature are presented in Fig. 7. As in the case of tungsten, silicon particles are strong scatterers so the extinction parameter is larger than the absorption parameter. Also electron micrographs indicate that the particles are nonspherical and are of various sizes. For the submicron-sized silicon particles investigated, $\mu_e \simeq 65{,}000$ cm²/g, essentially independent of λ from 1600 to 6000 Å.

Measurements of μ_e for tungsten particles in the size range from 0.1 to 0.2 μ in hydrogen at 12.5 atm. pressure at three temperatures are presented in Fig. 8. Data taken at pressures of 70, 100, and 115 atm for particles in the size range of 0.2 to 0.5 μ are presented by Fig. 9–11. The particles were larger at the higher pressures since a dispersion nozzle was not used above 12.5 atm. Since the Mie theory results change <3% over this temperature range, only their room temperature values were plotted. The magnitude of μ_e increases with temperature, and it increases most rapidly at the shorter wavelengths. This may be partially due to the effect of thermal agitation on the aerosol. As agglomerates are broken up into smaller particles, the Mie theory would predict a larger extinction parameter, particularly at the shorter wavelengths. Values of μ_e larger than those predicted by theory are not unreasonable, since the theory assumes spherical particles, and electron micrographs show the particles to be quite irregular in shape and to have a correspondingly larger surface area. Another effect which may be expected to increase μ_e at high temperatures is related to thermionic emission by the particles. The increase in the aerosol opacity at higher temperatures in the flash heating experiments conducted at McDonnell Douglas[23] was ascribed to thermionic emission from the particles. Measurements of the electrical conductivity of the aerosol substantiated this by showing that the conductivity increased substantially during the time of increased opacity. Theoretically, at sufficiently high temperatures, a metallic particle may become surrounded by a cloud of electrons which capture and emit photons by an inverse bremsstrahlung effect.[23] Thus, μ_e may increase whereas μ_a might actually be lowered due to the shielding effect of the electrons. Very little is known about the nature of such clouds of electrons which may surround thermionically emitting particles at high temperatures, particularly with respect to irregularly shaped submicron-sized particles in high pressure gases. It is clear from the measurements of μ_e for tungsten particles that there is an increase in μ_e at higher temperatures, and this effect is much more pronounced at higher pressures than at one atmosphere pressure.

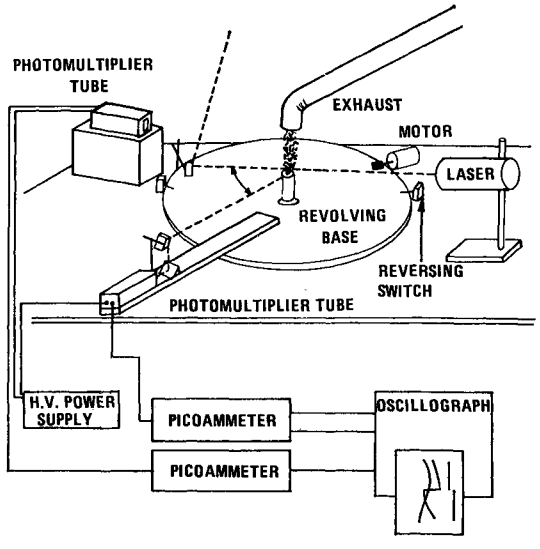

Fig. 12 Apparatus for scattering measurements.

Measurements of the Scattering Amplitude Function

The scattering amplitude function has an important effect on thermal radiation transport through particle clouds, especially if the particles are highly scattering. As was reported by Stockham and Love[24] regarding their Monte Carlo solution for a cylindrical particle cloud, "The results obtained indicate that anisotropic scattering plays an important role in heat transfer in this geometry. While Rayleigh scattering may still be closely approximated by isotropic scattering, the anisotropic scattering results may differ greatly from those assuming isotropic scattering."

The authors have measured the scattering amplitude function of submicron carbon, silicon, tungsten, tungsten carbide, and silicon carbide particles suspended in nitrogen at a wavelength of 6328 Å for scattering angles from 1° to 179° using the equipment illustrated by Fig. 12. A helium-neon laser beam was directed through an optically thin column of N_2 seeded with submicron refractory particles as it issued from a 0.5-in.-diam tube. The intensity of the light scattered from the particles was measured as a function of angle using a photomultiplier tube mounted on the revolving base. In

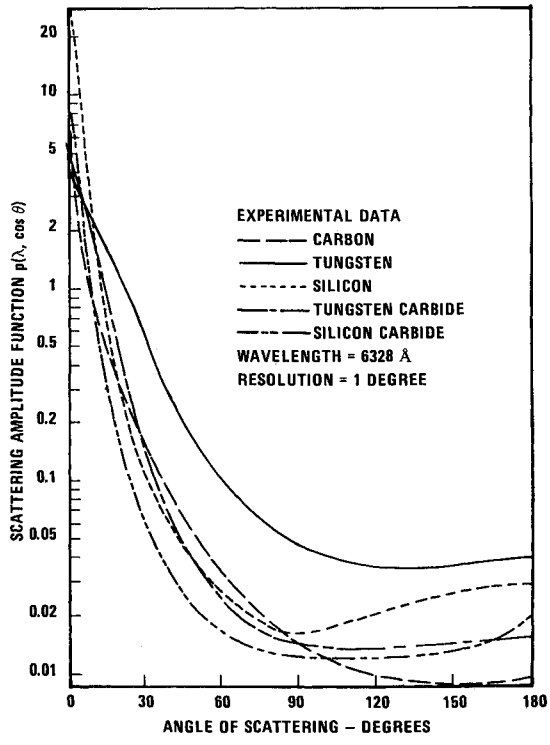

Fig. 13 Scattering amplitude functions of submicron refractory particles—experimental data.

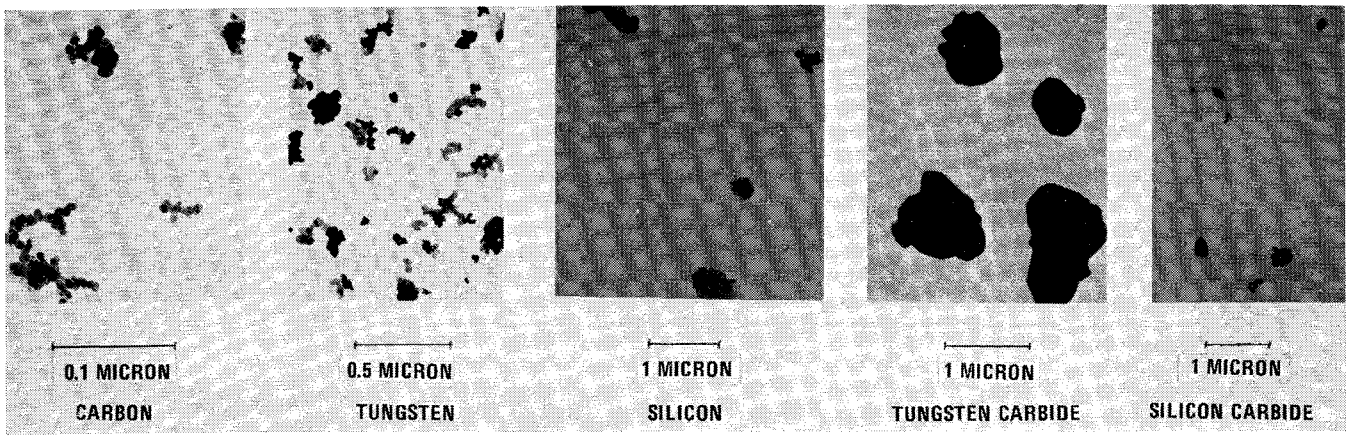

Fig. 14 Electron micrographs of submicron refractory particles.

order to account for fluctuations in the total number of scattering centers, a stationary photomultiplier was used to monitor continuously the intensity of light scattered at a fixed angle. The signals from these two photomultipliers were amplified and recorded simultaneously by an oscillograph. Since the intensity of the scattered light varied by several orders of magnitude, the signal from the moving photomultiplier was amplified by an automatic-ranging picoammeter. The value of the range was also recorded by the oscillograph.

The traverse of the moving photomultiplier was limited by two reversing switches. Data were taken by allowing the base to rotate through 180°, automatically reverse, and return to its original position. Two front surface mirrors were used in a periscope arrangement so that the laser beam would not be blocked by the photomultiplier tube housing as the observed angle of scattering approached 180°. A small mirror was also used to divert the laser beam after it passed through the aerosol in order to protect the photomultiplier tube from being damaged by the laser beam when the observed angle of scattering reached 0°.

For each run, data were also taken without particles in the gas in order to correct for light reaching the photomultipliers which was not scattered by the particles. The data for the aerosol were then analyzed by dividing the signal from the moving photomultiplier by the signal from the stationary photomultiplier to correct for fluctuations in the number of scattering centers in the beam during the 20 sec while data were being taken. The resulting data were normalized to unity in order to arrive at the scattering amplitude function. The results are presented vs angle of scattering in Fig. 13. Most of the scattered light is scattered at angles of $<30°$. Electron micrographs of the particles are presented in Fig. 14.

Discussion of Results

μ_e is easier to measure than μ_s, μ_a, or $p(\cos\theta)$ since all that is required is to measure the reduction of intensity of a beam of radiant energy by an aerosol of known particle concentration. μ_s may be evaluated by measuring the total scattered energy by an optically thin particle cloud of known particle concentration. μ_a may be found by subtracting μ_s from μ_e; it cannot be measured directly by optical means.

When particle seeding is used to enhance radiant heat transfer to a gas, it is essential that μ_a be as large as possible since scattered energy does not heat the particles. Nonconducting particles (such as AlO in Fig. 1) have low values of μ_a and are not useful for this purpose. The high values of both μ_a and μ_e indicate that aerosols of the submicron refractory metal particles investigated are highly effective for thermal radiation shielding and to enhance radiant heat transfer to gases. For the gas core nuclear rocket, tungsten now appears to be the best seed material. Carbon particles react with hydrogen and therefore would not be useful for this application.

The increase in μ_e of tungsten-hydrogen aerosols at high temperatures and pressures indicates that the amount of seed material required for the gas core nuclear rocket may be much less than had been previously thought based on measurements at 1 atm pressure. It is not yet known how much of this increase in μ_e is due to an increase in μ_a and how much is due to an increase in μ_s.

The effect of scattering depends not only on μ_s but also on the angular dependence of the scattered energy as represented by $p(\cos\theta)$. Forward scattering particles are less effective in diffusing radiant energy than particles which tend to scatter at larger angles. The measured values of the scattering amplitude functions of aerosols of submicron-sized refractory particles illustrate the highly forward nature of scattering from these particles.

References

[1] Howell, J. R. and Renkel, H. E., "Analysis of the Effects of a Seeded Propellant Layer on Thermal Radiation in the Nozzle of a Gaseous Core Nuclear Propulsion System," TN-D-3119, 1962, NASA.

[2] Rom, F. E., "Comments on the Feasibility of Developing Gas Core Nuclear Reactors," TM-X-52644, Oct. 1969, NASA.

[3] Ragsdale, R. G. and Lanzo, C. D., "Some Recent Gaseous Reactor Fluid Mechanics Experiments," AIAA Paper 69-477, U.S. Air Force Academy, Colo., 1969.

[4] Clark, J. W. et al., "Open-Cycle and Light Bulb Types of Vortex-Stabilized Gaseous Nuclear Rockets," *Journal of Spacecraft and Rockets*, Vol. 5, No. 8, Aug. 1968, pp. 941–947.

[5] Rosa, R. J., *Magnetohydrodynamic Energy Conversion*, McGraw-Hill, New York, 1968, pp. 180–195.

[6] Williams, J. R., Kallfelz, J. M., and Shelton, S. V., "A Parametric Survey of Gas Core Reactor-MHD Power Plant Concepts," *Proceedings of the 5th Intersociety Energy Conversion Engineering Conference*, Las Vegas, Nevada, Sept. 1970.

[7] Keyes, J. J., Jr. and Sartory, W. K., "A Study of Nuclear-Magnetohydrodynamic Central-Station Power Generation," Rept. ORNL-TM-3101, March 1966, Oak Ridge National Lab.

[8] Mitchel, B. J., "Re-Entry Radiation Shielding by a Boundary Layer Precipitate," AIAA Paper 70-156, New York, 1970.

[9] Lanzo, C. D. and Ragsdale, R. G., "Experimental Determination of Spectral and Total Transmissivities of Clouds of Small Particles," TN-D-1405, Sept. 1962, NASA.

[10] Keng, E. and Orr, C., "Investigation of Radiant Heat Transfer to Particle-Seeded Gases for Application to Nuclear Rocket Engine Design," CR-953, Nov. 1967, NASA.

[11] Burkig, V. C., "Thermal Absorption in Seeded Gases," Rept. DAC-59985, NASw-1310, Jan. 1967, Donald W. Douglas Labs.

[12] Klein, J. F. and Roman, W. C., "Results of Experiments to Simulate Radiant Heating of Propellant in a Nuclear Light Bulb Engine Using a D-C Arc Radiant Energy Source," Rept. J-910900-1, Sept. 1970, United Aircraft Research Labs.

[13] Love, T. J., "An Experimental Investigation of Infra-red Scattering by Clouds of Particles," Rept. ARL-64-109, June 1964, Aerospace Research Labs.

[14] Williams, J. R., "Thermal Radiation Transport in Particle-Seeded Gases," *ANS Transactions*, Vol. 12, Dec. 1969, pp. 811–812.

[15] Mie, G. A., "Beitrage zur Optik truber Medien, Speziell Kolloidaler Metallosungen," *Annalen Der Physik*, Vol. 25, No. 3, 1908, pp. 377–445.

[16] Krascella, N. L., "Theoretical Investigations of the Absorption and Scattering Characteristics of Small Particles," Rept. C-910092-1, Sept. 1964, United Aircraft Research Labs.

[17] Aden, A. L., "Electromagnetic Scattering from Spheres with Sizes Comparable to the Wavelength," *Journal of Applied Physics*, Vol. 22, No. 5, 1951, pp. 601–605.

[18] Williams, J. R., Shenoy, A. S., and Clement, J. D., "Theoretical Calculations of Radiant Heat Transfer Properties of Particle-Seeded Gases," CR-1505, Feb. 1970, NASA.

[19] Plass, G. N., "Mie Scattering and Absorption Cross Sections for Aluminum Oxide and Magnesium Oxide," *Applied Optics*, Vol. 3, No. 7, 1964, pp. 867–872.

[20] Chi, J. W. H. and Landahl, C. E., "Hydrogen Reactions with Graphite Materials at High Temperatures and Pressures," *Nuclear Applications*, Vol. 4, March 1968, pp. 159–169.

[21] Clarke, J. T. and Fox, B. R., "Reaction of Graphite Filaments with Hydrogen above 2000°K," *Journal of Chemical Physics*, Vol. 46, No. 3, Feb. 1967, pp. 827–836.

[22] Duff, R. E. and Bauer, S. H., "Equilibrium Composition of the C/H Systems at Elevated Temperatures," *Journal of Chemical Physics*, Vol. 36, No. 7, April 1962, pp. 1754–1767.

[23] Cory, J. S. and Bennett, A., "Thermal Absorption in Seeded Gases," Rept. DAC-60779, Feb. 1969, Donald W. Douglas Labs.

[24] Stockham, L. W. and Love, T. J., "Monte Carlo Solution of Radiative Heat Transfer from a Finite Cylindrical Cloud of Particles," AIAA Paper 68-64, New York, 1968.

APRIL 1971 J. SPACECRAFT VOL. 8, NO. 4

Two-Dimensional Analysis of Transonic Gas-Particle Flows in Axisymmetric Nozzles

JOSEPH F. REGAN,* H. DOYLE THOMPSON,† AND RICHARD F. HOGLUND‡
Purdue University, Lafayette, Ind.

A recently developed two-dimensional technique for the calculation of isentropic perfect gas flowfields in axisymmetric nozzles of sharp wall curvature is used to provide initial values for a two-phase transonic flowfield calculation. The governing equations for the two-phase flow are expressed as finite-difference replacement equations that are solved by a numerical relaxation technique. A particle-free region appears and grows along the nozzle walls; the gas expansion in this region is regarded as isentropic to the predetermined local value of static pressure. Calculated flowfields and particle trajectories are presented for two families of nozzle contours and three particle sizes, and compared with the frequently employed constant-fractional-lag-mixture (CFLM) assumption and with calculations[6] based on a combination of the Sauer approximation to transonic flows and the CFLM assumption. Appreciable differences are found, especially in near-wall regions. The propagation of these differences through the supersonic nozzle flow is demonstrated.

Nomenclature

C_d = particle drag coefficient
C_P = specific heat at constant pressure
D = diameter
F = variable particle drag factor
G = variable particle heat-transfer factor
m = density per unit volume of particle
M = Mach number
P = pressure
R = gas constant
Re = Reynolds number
Rs = ratio of nozzle wall radius of curvature to throat radius
T = temperature
u = x-direction gas velocity component
v = y-direction gas velocity component
W = speed
x = axial coordinate along nozzle axis
y = radial coordinate measured from nozzle axis
γ = isentropic exponent
θ = streamline angle with respect to nozzle axis
μ = viscosity coefficient
ρ = density per unit volume of gas-particle mixture
Φ = particle-to-gas mass flow ratio

Subscripts§

g = gas property
o = total condition
p = particle property

Presented as Paper 69-572 at the AIAA 5th Propulsion Joint Specialist Conference, U.S. Air Force Academy, Colo., June 9–13, 1969; submitted October 20, 1969; revision received August 26, 1970. The authors gratefully acknowledge the assistance of G. Johnson of Purdue University, who made the supersonic nozzle performance calculations using the TRW computer program, and T. F. Zupnik of Pratt and Whitney Aircraft, who provided the perfect gas transonic flow program and useful consultation in understanding its logic and operation. Appreciation is also extended to J. D. Hoffman of Purdue University for his stimulating discussions throughout the course of the investigation.

* Colonel, U.S. Air Force; presently Director, Ramjet Division, Aero Propulsion Laboratory, Wright-Patterson Air Force Base, Ohio.

† Associate Professor of Mechanical Engineering. Member AIAA.

‡ Associate Professor and Director of Project SQUID; presently Manager, Physics and Applied Mechanics Department, Atlantic Research Corporation, Alexandria, Va. Associate Fellow AIAA.

§ Sub-subscript x or y denotes differentiation.

Introduction

IT now has been established both theoretically[1] and experimentally[2] that neither one-dimensional calculation techniques nor attempts to introduce two-dimensionality, via